

Metatranscriptomic response of deep ocean microbial populations to infusions of oil and/or synthetic chemical dispersant

Tito D. Peña-Montenegro,^{1,2,3} Sara Kleindienst,¹ Andrew E. Allen,^{4,5} A. Murat Eren,^{6,7} John P. McCrow,⁴ Jonathan Arnold,^{2,8} Samantha B. Joye¹

AUTHOR AFFILIATIONS See affiliation list on p. 15.

ABSTRACT Oil spills are a frequent perturbation to the marine environment that has rapid and significant impacts on the local microbiome. Previous studies have shown that exposure to synthetic dispersant alone did not enhance heterotrophic microbial activity or oxidation rates of specific hydrocarbon components but increased the abundance of some taxa (e.g., *Colwellia*). In contrast, exposure to oil, but not dispersants, increased the abundance of other taxa (e.g., *Marinobacter*) and stimulated hydrocarbon oxidation rates. Here, we advance these findings by interpreting metatranscriptomic data from this experiment to explore how and why specific components of the microbial community responded to distinct organic carbon exposure regimes. Dispersant alone was selected for a unique community and for dominant organisms that reflected treatment- and time-dependent responses. Dispersant amendment also led to diverging functional profiles among the different treatments. Similarly, oil alone was selected for a community that was distinct from treatments amended with dispersants. The presence of oil and dispersants with added nutrients led to substantial differences in microbial responses, likely suggesting increased fitness driven by the presence of additional inorganic nutrients. The oil-only additions led to a marked increase in the expression of phages, prophages, transposable elements, and plasmids (PPTs), suggesting that aspects of microbial community response to oil are driven by the “mobilome,” potentially through viral-associated regulation of metabolic pathways in ciliates and flagellates that would otherwise throttle the microbial community through grazing.

IMPORTANCE Microcosm experiments simulated the April 2010 Deepwater Horizon oil spill by applying oil and synthetic dispersants (Corexit EC9500A and EC9527A) to deep ocean water samples. The exposure regime revealed severe negative alterations in the treatments’ heterotrophic microbial activity and hydrocarbon oxidation rates. We expanded these findings by exploring metatranscriptomic signatures of the microbial communities during the chemical amendments in the microcosm experiments. Here we report how dominant organisms were uniquely associated with treatment- and time-dependent trajectories during the exposure regimes; nutrient availability was a significant factor in driving changes in metatranscriptomic responses. Remarkable signals associated with PPTs showed the potential role of mobilome and viral-associated survival responses. These insights underscore the time-dependent environmental perturbations of fragile marine environments under oil and anthropogenic stress.

KEYWORDS *Colwellia*, *Marinobacter*, deepwater horizon oil spill, Corexit, metatranscriptome, mobilome, giant virus

Editor Jennifer F. Biddle, University of Delaware, Lewes, Delaware, USA

Address correspondence to Samantha B. Joye, mjoye@uga.edu.

The authors declare no conflict of interest.

See the funding table on p. 16.

Received 6 June 2024

Accepted 6 June 2024

Published 23 July 2024

[This article was published on 23 July 2024 with a statement missing from Acknowledgments. The Acknowledgments were corrected in the current version, posted on 26 July 2024.]

Copyright © 2024 Peña-Montenegro et al. This is an open-access article distributed under the terms of the [Creative Commons Attribution 4.0 International license](https://creativecommons.org/licenses/by/4.0/).

Oil spills occur frequently in the marine environment, sometimes with calamitous consequences (1). Most marine oil spills have involved accidents in the coastal ocean (e.g., Exxon Valdez and MC20 Taylor Energy accidents) (2, 3), but offshore spillage of oil occurs as well, via operational discharges and drilling accidents, e.g., the Ixtoc oil well blowout in Mexico in 1979 (3) and the Deepwater Horizon (DWH) oil well blowout in the Gulf of Mexico in 2010 (1). The DWH oil disaster resulted from a massive explosion following the discharge of hydrocarbons, which continued for 84 days and released approximately 4.9 million barrels of oil and around 250,000 metric tons of natural gas into the Gulf of Mexico at a depth of 1,500 m. Such discharges provide acute, chronic, or pulsed inputs of oil into the marine environment that lead to modifications in the structure of marine microbial communities and can substantially alter microbial community function (1).

Given the magnitude of the DWH oil spill, synthetic chemical dispersants were used (4), both at the discharging wellhead and along surface oil slicks, as a response measure to move the oil from the organic phase (slick, discharge plume) to the aqueous phase to minimize environmental damage (e.g., oiled beaches and marshes) and accelerating microbial oil biodegradation via the creation of small droplets with enhanced bioavailability (4). Synthetic chemical dispersants comprise petroleum distillates and non-ionic and anionic surfactants (5). These organic substrates are extremely labile, offering microbial populations an organic carbon source to fuel their metabolism (6, 7). Some 7 million liters of synthetic dispersant was applied in response to the DWH oil spill—2.9 million liters was applied at the discharging wellhead at the seabed—and while it is clear that synthetic dispersants altered microbial communities and potentially slowed oil degradation (8), exactly how dispersant-derived organic carbon modulated this response is unknown.

This work builds on the foundational work of Kleindienst et al. (9), which simulated the environmental conditions in the hydrocarbon-rich 1,100-m deepwater plume that formed during the DWH spill. In the Kleindienst et al. experiment (9), deep water (~200 L) from about 1,400-m water depth above an oil plume at a natural oil seep site (Green Canyon 600 in the Northern Gulf of Mexico) was collected on board a research vessel and returned to the laboratory for manipulation in a laboratory experiment. Several reports were generated from the Kleindienst et al. experiment (9), showing (i) changes in oil composition across treatments (10), (ii) patterns of the microbial production of transparent exopolysaccharides across treatments (11), and (iii) species-specific adaptations of *Marinobacter* and *Colwellia*, two key microbial responders to oil and dispersant infusions using metatranscriptomic data in the context of pangenomes (12). We used metatranscriptomic data collected from the Kleindienst et al. experiment to compare and contrast community-level expression signatures to reveal how microbial communities responded to distinct organic carbon exposure regimes of synthetic dispersants and/or oil.

The Kleindienst et al. experiment (9) involved exposing replicate ($n = 3$) microcosms to a matrix of controlled conditions to isolate the community response to oil versus dispersant exposure. Treatments were amended with a water-accommodated fraction (WAF) of oil-only, the synthetic dispersant (DISP) Corexit 9500, oil and Corexit mixtures (i.e., chemically enhanced water-accommodated fraction — CEWAF), and CEWAF plus nutrients (CEWAFN). The response of Gulf deepwater microbial populations to these additions was tracked over five time points in a span of 6 weeks ($t_0 = 0$, $t_1 = 7$, $t_2 = 17$, $t_3 = 28$, and $t_4 = 42$ days), while replicate samples were sacrificed to assess microbial community composition, microbial activity, chemistry, and metatranscriptomics. Here, we advance the findings of Kleindienst et al. (9) by interpreting metatranscriptomic data from their experiment to explore how and why specific components of the microbial community responded to distinct exposure regimes.

RESULTS

Transcriptomic libraries ($n = 27$) ranged in size from 4.6 to 18.75 million reads, with a mean of 10.58 million reads per sample and an average read length of 97 bp. About 44.38% of reads remained after quality control and removal of sequencing artifacts and duplicates (Fig. S1A). Predicted features were assigned to 68% of these reads, while 2.74% were associated with rRNA transcripts (Fig. S1B). In total, 11.3 million reads (30.18% of the initial reads) mapped taxonomic features with an average of 1,638 reads assigned to archaea, 403,781 reads assigned to bacteria, 5,357 reads assigned to eukaryotes, and 10,542 reads assigned to viruses (Fig. S2; Supplemental Data 1). Roughly 3.1 million reads per library were annotated at the functional level.

We observed significant differences in species diversity across treatments [one-way analysis of variance (ANOVA), $R^2 = 0.21$, $P < 0.0001$]. Except for the biotic control and dispersant treatments, the samples showed differences of more than 1,000 species between the early stages of the experiment (t_0 and t_1) and the end of the experiment (t_4), possibly driven to some degree by limitations in sequencing depth or inherent variability on diversity richness at a given sample (Fig. S3). For instance, using a sampling depth of 13.9 million reads as the cutoff, after 42 days of dispersant exposure, only ~4,095 species were recovered (i.e., α -diversity = 27); this was the lowest number compared to the WAF (~5,000 species), CEWAF (~6,000 species) and CEWAFN (~5,000 species) treatments (Fig. S3). Additionally, the α -diversity index for the CEWAF \pm nutrient treatments increased over time, while the rest of the treatments declined over time (Fig. S3F).

Exposure to synthetic dispersants generated taxa-specific responses in expression that modulated the community response to different chemical combinations of oil and/or dispersant. The taxonomic profile of the active population identified by the annotated transcripts resembled the community structure shown through 16S rRNA gene sequencing (9). All dispersant-amended samples showed significant transcriptional enrichment for *Colwellia* (t -test, $P < 0.0001$), an organism known for its role in hydrocarbon and dispersant degradation (13). After one week, the relative abundance of *Colwellia* transcripts increased from 3.9%–7.4% to 71.4%–79.6% in dispersant-only and CEWAF \pm nutrient treatments (Fig. 1) and from 7.2% to 26.3%–34.9% in WAF treatments. *Colwellia* increased by 30.6% in gene expression compared to a 2.5% increase in abundance (16S rRNA gene counts) in the WAF treatment. *Marinobacter* accounted for a significant increase of transcriptional signals in WAF treatments compared to the rest of the treatments (t -test, $P = 0.0206$), with a relative increase from 7.0% to 18.7%–52.5% after 4 weeks (Fig. 1). In dispersant-only and CEWAF \pm nutrient treatments, *Marinobacter* transcripts decreased from 6.0%–9.0% to 0.5%–0.8%. After the first week, the *Colwellia* transcriptomic response declined in WAF treatments, while that of *Marinobacter* increased. After 6 weeks of dispersant-only exposure, increased expression (up by 46.8%) by *Kordia* was observed; this relative increase was far more pronounced than the relative 16S rRNA gene counts of *Kordia* (up by 11.8%) (9). Although the difference in *Kordia* proportions (metatranscriptomic versus 16S signals) was not significant (t -test, $P = 0.243$), their trends over time showed significant differences (least square fit significant parameters, dispersant $P = 0.0068$, time $P = 0.0134$, dispersant \times time $P = 0.0003$).

The ratio of total RNA to DNA has been proposed as an estimator for multiple physiological parameters (i.e., tissue development, growth fitness, and effective phenotype) (14). Here, we calculated the mean log-transformed RNA:DNA (LRD) ratio as an approach to describe the level of effective transcriptional activity (i.e., synthetic capacity) between transcriptomic and 16S rRNA gene signals (9) across treatments. The largest fraction of relative counts at the transcriptomic and 16S rRNA gene level were distributed proportionately across treatments (Fig. 2, Group II: |mean LRD| ≤ 3.5), including hydrocarbon degraders such as *Marinobacter* and *Colwellia*. The group of organisms that had a larger relative synthetic capacity (Fig. 2, Group I: mean LRD > 3.5) was composed of members associated typically with methylotrophic metabolism (*Methylophaga* and *Methylobacter*), oil influence (*Bermanella*), hydrocarbon degradation (*Pseudomonas*), and

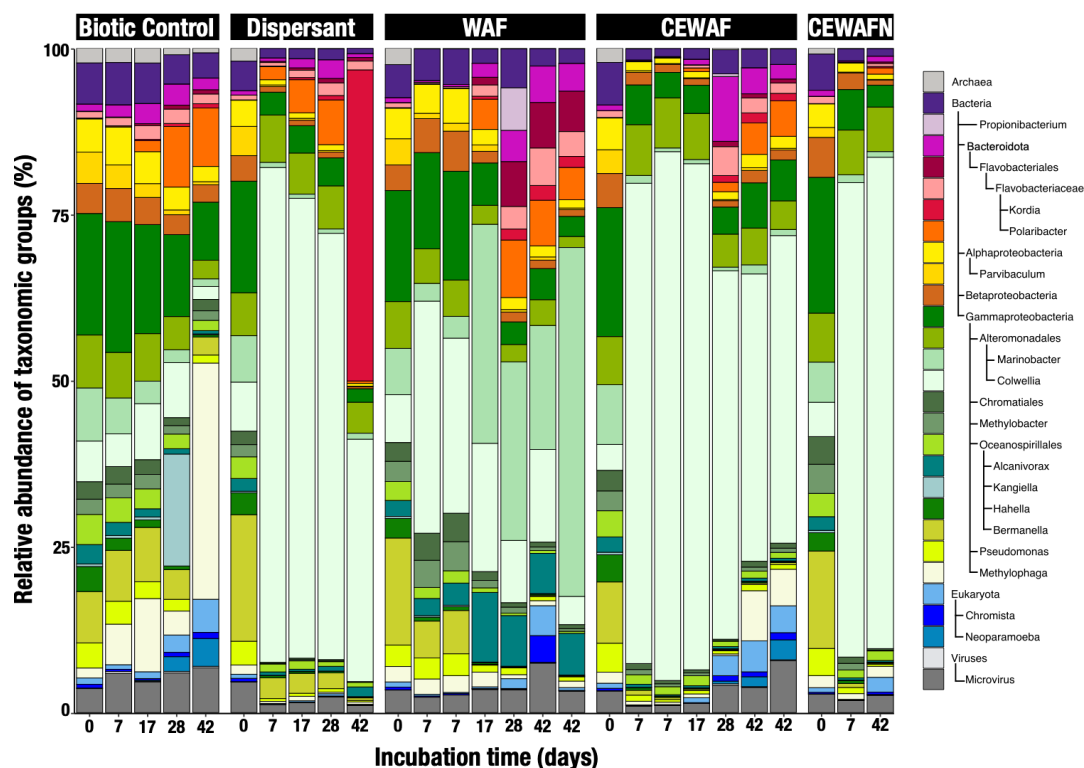


FIG 1 Relative abundance of merged taxonomic ranks in the Kleindienst et al. metatranscriptomic libraries at a minimum allowed resolution of 4% based on taxonomy assignment performed in MG-RAST.

alkylbenzenesulfonate degradation (*Parvibaculum*) (15). Organisms with a low LRD index (Fig. 2, Group III: mean LRD < -3.5) included members of the family *Oceanospirillaceae*, such as *Amphritea*, *Pseudospirillum*, and *Balneatrix*; hydrocarbon degraders, including *Oleiphilus*, *Porticoccus*, and *Cycloclasticus*; as well as members of *Flavobacteria*, including *Bacteroidota*, *Pseudobdellovibrionaceae*, and *Spongibacter*. All LRD values presented in this analysis showed a significant correspondence across taxa (one-way ANOVA, $R^2 = 0.97$, $P < 0.0001$).

Beta-diversity was assessed via Bray-Curtis dissimilarity-based principal component analysis (PCA) of metatranscriptomic reads (Fig. 3A). Consistent with the taxonomic profile (Fig. 1), all treatments amended with dispersants were positively correlated with *Colwellia*. Oil-only samples occupied a separate cluster transitioning from a broad positive association with *Gammaproteobacteria* to a positive association with *Marinobacter* specifically. A third cluster comprising the biotic control spanned a positive association with *Gammaproteobacteria* with small positive contributions from *Marinobacter*, *Bacteroidota*, *Polaribacter*, *Flavobacteriales*, and *Alcanivorax*.

The interaction of oil \pm dispersants and time was correlated significantly with changes in phylogenetic distances associated with the evolution of the microbial community. We performed a permutational multivariate analysis of variance on (i) taxonomic dissimilarity (i.e., Bray-Curtis) distances and (ii) phylogenetic dissimilarity via weighted mean pairwise distances (MPDs) and weighted mean nearest taxon distances (MNTDs). Dispersant ($R^2 = 0.27$, $P = 0.001$) and time ($R^2 = 0.18$, $P = 0.001$) terms significantly explained the variability of the Bray-Curtis distance profile. Similarly, dispersant ($R^2 = 0.09$, $P = 0.001$), time ($R^2 = 0.06$, $P = 0.015$), and dispersant \times time ($R^2 = 0.05$, $P = 0.037$) explained the MPD phylogenetic distance profile. In contrast, oil \times time ($R^2 = -0.17$, $P = 0.010$) and dispersant \times oil \times time ($R^2 = -0.59$, $P = 0.005$) explained the MNTD phylogenetic distance profile, indicating that higher levels of dissimilar transcriptional responses were observed in dispersant treatments and over time. By weighting transcriptional abundances and phylogenetic proximity among taxa, we observed that the interaction

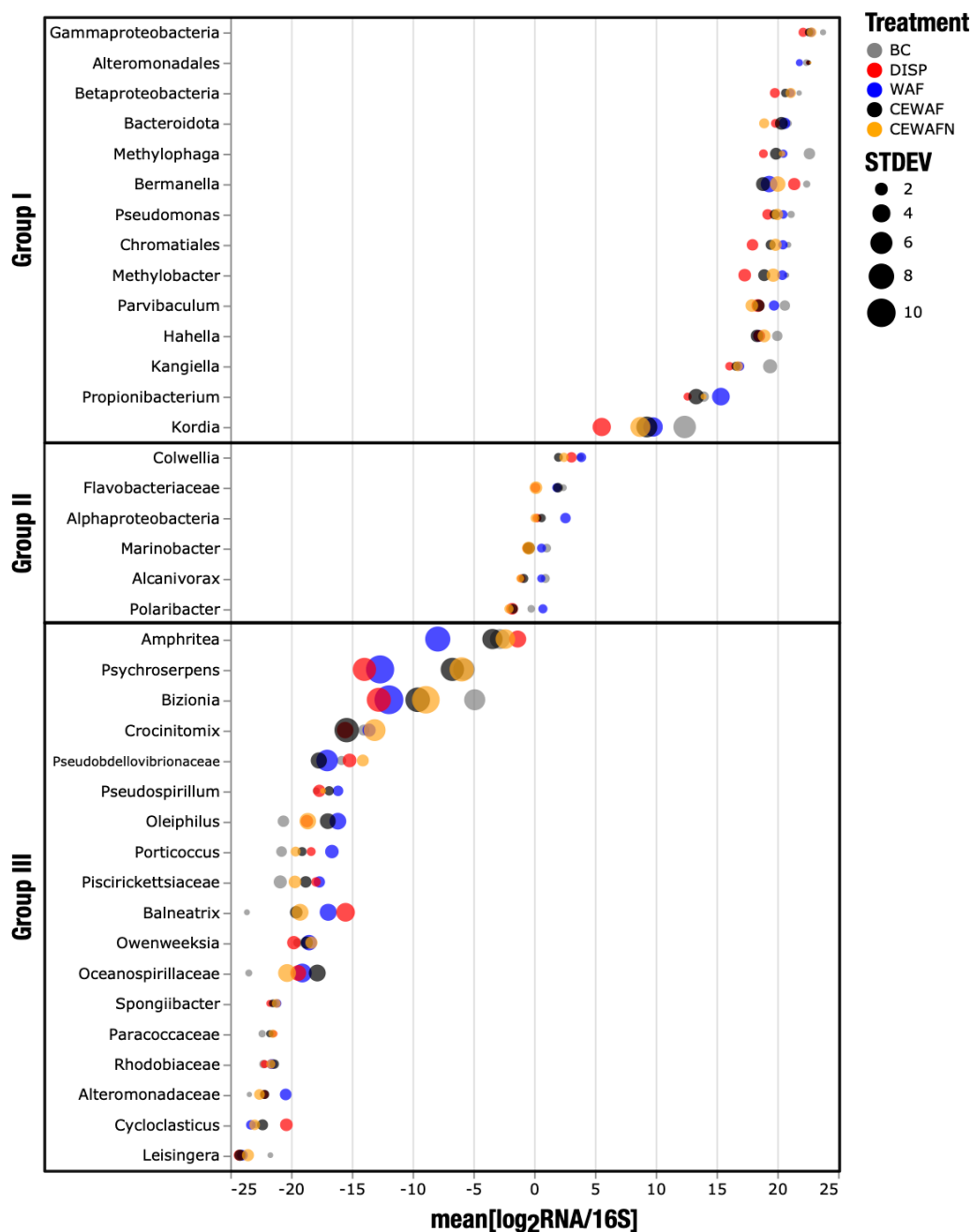


FIG 2 Indigenous hydrocarbon degraders are consistently found in 16S rRNA gene sequences as well as in transcriptomic libraries. LRD ratio distribution across Kleindienst et al. metatranscriptomic libraries. Taxonomic groups are sorted from top to bottom by descending mean of LRD scores. Biosynthetic capacity is expected to be the greatest in Group I (mean LRD >3.5), followed by Group II (|mean LRD| ≤3.5), and the smallest for Group III (mean LRD <-3.5). LRD, log-transformed RNA:DNA; BC, biotic control; DISP, dispersant; WAF, oil; CEWAF, dispersant + oil; CEWAFN, CEWAFN, CEWAF + nutrients; STDEV, standard deviation.

terms oil × time and dispersant oil × time became significant for explaining MNTD dissimilarity distances in the data set. Additionally, we observed shifts of time-dependent trends of pathways in dispersant-only versus chemically enhanced water-accommodated oil fraction with or without nutrient treatments (Fig. S5 and S6).

In the first 2 weeks after chemical exposure, the CEWAF treatment exhibited a relative expression increase in 20 functional categories (Fig. 4; Fig. S4), including “secondary

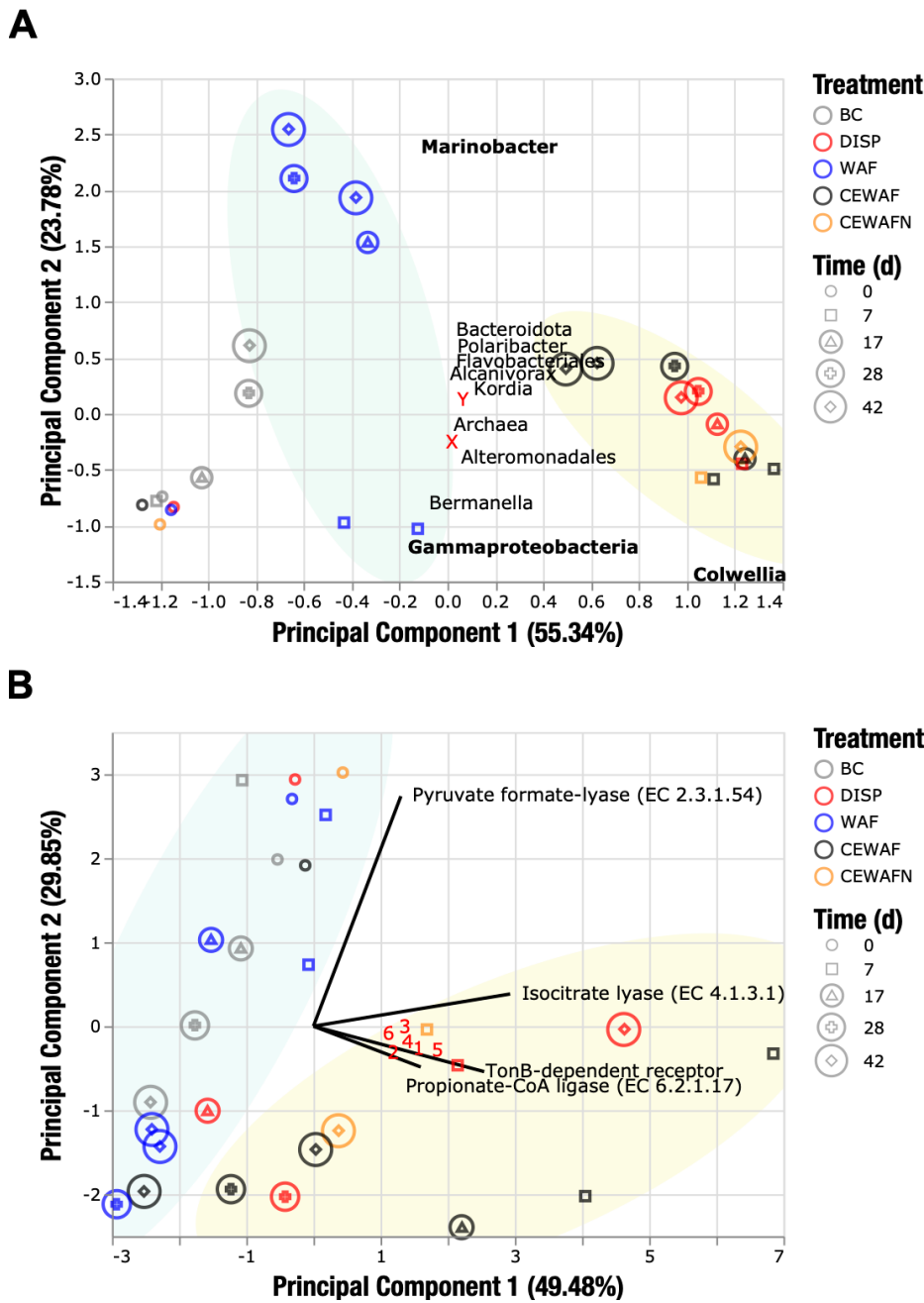


FIG 3 Diversity and functional dimensional analysis of the Kleindienst et al. metatranscriptomic data set. (A) Principal coordinate analysis of relative abundance of taxonomic groups. Near the X label, we found the following microbial groups: *Alphaproteobacteria*, *Betaproteobacteria*, *Oceanospirillales*, *Methylobacter*, *Parvibaculum*, *Chromatiales*, and *Hahella*. Near the Y label, we found the following microbial groups: *Neoparamoeba*, *Kangiella*, *Methylophaga*, *Chromista*, *Propionibacterium*, and *Microvirus*. (B) Functional expression of gene abundances assigned to the Subsystems for the Environmental and Ecological Data (SEED) subsystems: motility and chemotaxis, carbohydrates, membrane transport, and respiration. Solid lines represent the top 10 loading vectors explaining the expression signal variability in the analysis. Numbers in red are as follows: 1, 2-methylcitrate dehydratase FeS (EC 4.2.1.79); 2, acetoacetyl-coenzyme A reductase (EC 1.1.1.36); 3, aconitate hydratase 2 (EC 4.2.1.3); 4, acetolactase synthase large subunit (EC 2.2.1.6); 5, acetyl-coenzyme A synthetase (EC 6.2.1.1); and 6, malate synthase G (EC 2.3.3.9).

metabolism," "motility and chemotaxis," "dormancy and sporulation," "sulfur metabolism," and "stress response" categories. These enriched categories ranged around ~300,000 to over 1 million mapping reads at peak expression across treatments (Fig. 4). In contrast,

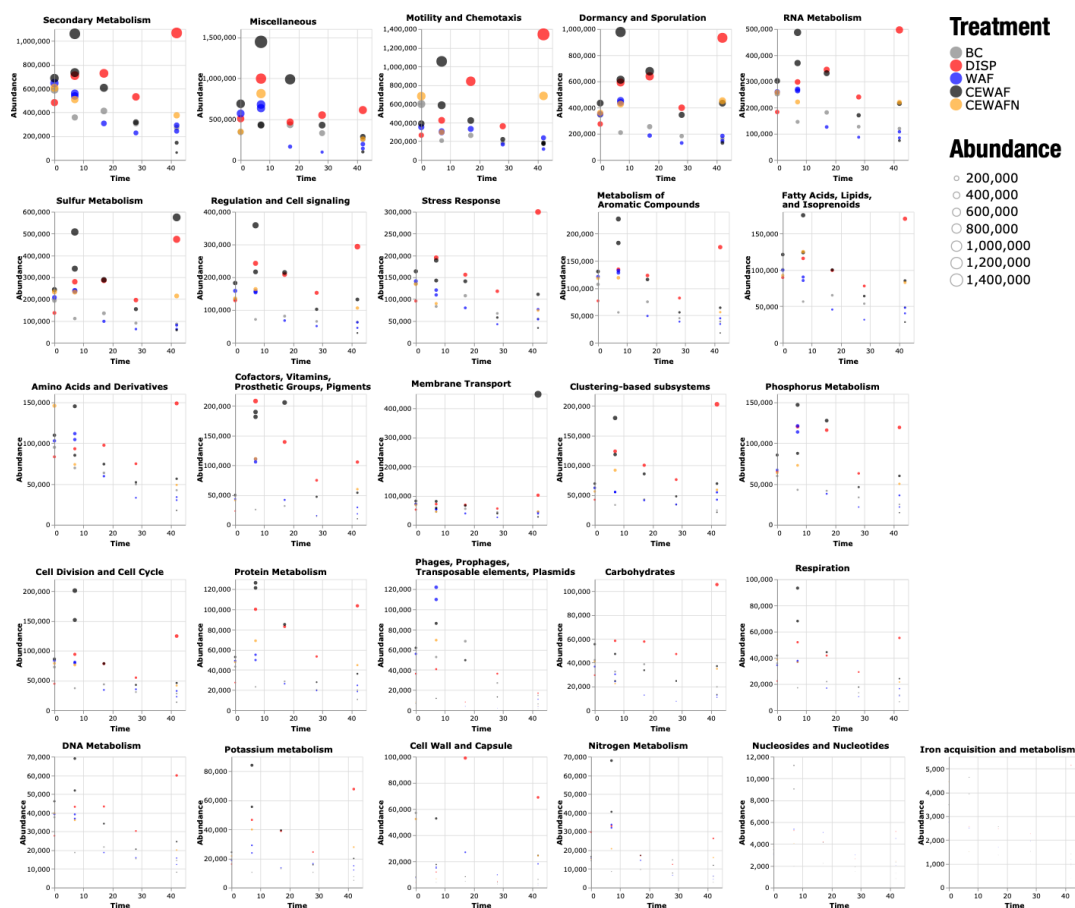


FIG 4 Abundance of gene expression based on automated SEED subsystems in MG-RAST for the Kleindienst et al. metatranscriptomic data set. Observations are color-coded by treatment. Dot sizes are proportional to the absolute abundance in a library. BC, biotic control; DISP, dispersant; WAF, oil; CEWAF, dispersant + oil; CEWAFN, CEWAF + nutrients.

the dispersant treatment showed a delayed transcriptional response in the same categories. In 17 out of 20 categories, two behaviors occurred: (i) a fast, strong response near t_1 and then a decay for the CEWAF treatment, and (ii) a slow incremental response with a maximum peak at t_4 for the dispersant treatment. “Phages, prophages, transposable elements, and plasmids” were the only functional category where the oil-only treatment showed the largest relative expression peak across treatments. These results would suggest transcriptional responses acting simultaneously upon several metabolic functions of the community. In contrast, other functional categories showed different transcriptional profiles. For instance, phages, prophages, transposable elements and plasmids were the only functional group where the WAF treatment reached the largest relative abundance after 1 week of incubation. The “cell wall and capsule” category showed the largest relative abundance for the dispersant-only treatment at t_3 and t_4 .

Here we also observed a strong signature expression of the *rebH* (DISP P value_{adj} = 0.001, WAF P value_{adj} = 0.001, CEWAF P value_{adj} = 0.001, and CEWAFN P value_{adj} = 0.003) and *prnA* (DISP P value_{adj} = 0.038, WAF P value_{adj} = 0.025, CEWAF P value_{adj} = 0.012, and CEWAFN P value_{adj} = 0.018) genes, coding for a flavin-dependent tryptophan halogenase (member of the secondary metabolism category) at the early stages of the experiment and with higher abundance for all dispersant amended treatments. All differentially expressed (DE) *rebH* and *prnA* transcripts were assigned to *Pelagibacter* phages, cyanobacteria-host phages, and *Colwellia* sp. MT41. The role of tryptophan halogenase, a precursor of the antibiotic pyrrolnitrin, suggests competition mechanisms

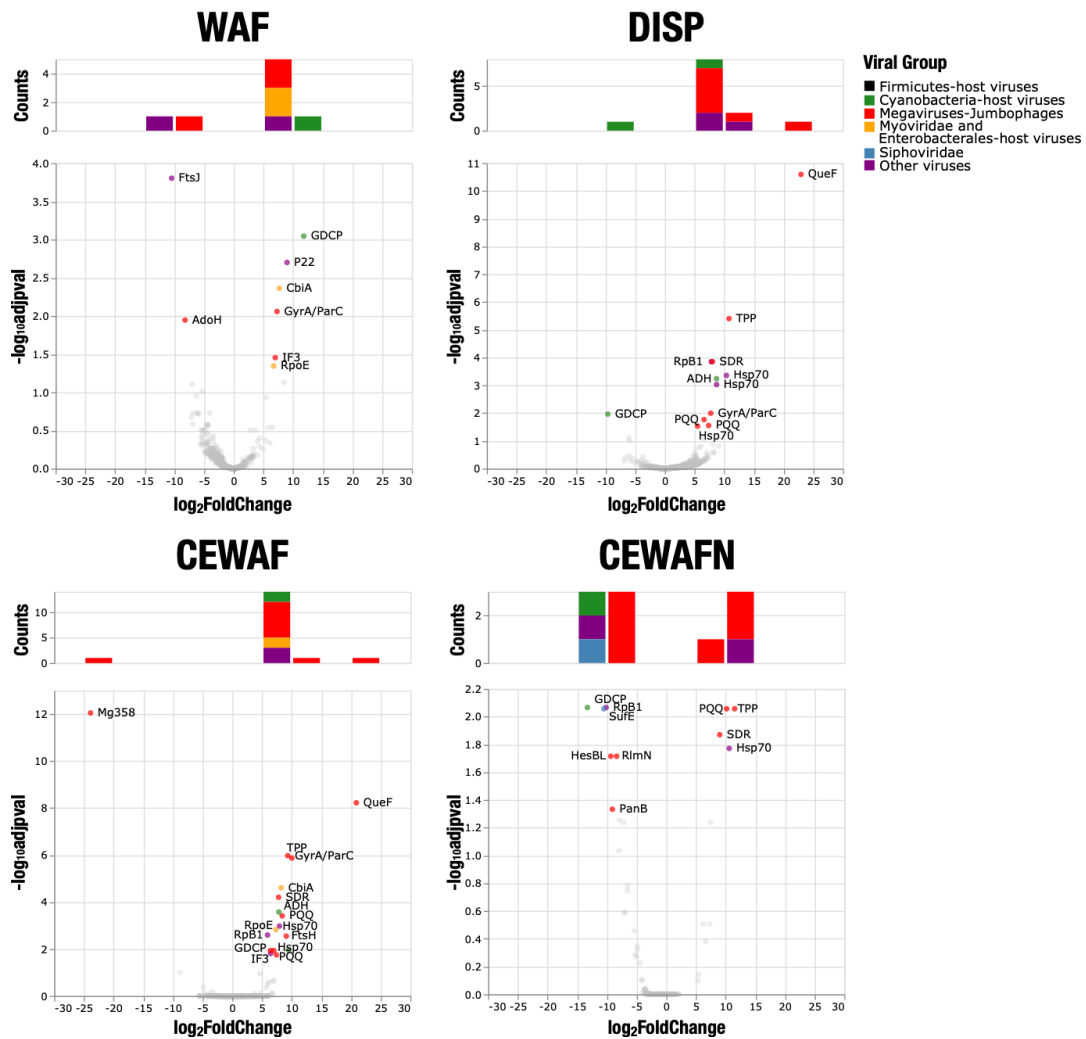


FIG 5 Volcano plots of genes assigned to viruses or prophages. Genes with P value_{adj} of <0.5 were considered as differentially expressed and are highlighted with their assigned functional and viral groups. Histograms on top of each volcano plot represent the distribution of DE genes by viral group and \log_2 Fold-Change. The two most common DE genes were Hsp70 ($n = 6$) and PQQ ($n = 6$), although several genes were frequently perturbed across treatments (e.g., GDCP $n = 4$, SDR $n = 3$, TPP $n = 3$, and RpB1 $n = 3$).

for *Colwellia* and surrounding viral and phage-controlled microbial members (Supplemental Data 1).

To further assess the influence of the chemical exposure on the metabolic variation among the metatranscriptomes, a PCA of the functional feature abundance across the SEED annotation levels was conducted (Fig. 3B and 4). Dispersant-amended samples showed a clustering pattern separated from the WAF and biotic controls at the level of functions of major non-housekeeping modules (Fig. 3B). Biotic control and WAF libraries showed similar clustering trends along the pyruvate formate lyase (PFL) (EC 2.3.1.54) loading vector. Higher expression of PFL was strongly associated with the t_0 libraries. On the other hand, CEWAF (t_1 and t_2) and dispersant (t_4) samples showed a strong positive association with PC1, supported by the contribution of isocitrate lyase (EC 4.1.3.1), TonB-dependent receptor (TBDR), propionate-coenzyme A ligase (EC 6.2.1.17), and other features involved in the biosynthesis of amino acids; biosynthesis of storage compounds (i.e., polyhydroxybutanoate biosynthesis via acetoacetyl-coenzyme A reductase EC 1.1.1.36); generation of metabolite and energy precursors; and degradation of carboxylates, carbohydrates, and alcohols.

Dispersants and CEWAF treatments showed similar trends in contrast to the unique pattern in the oil-only treatment. This observation was consistent across SEED annotation levels and subsets of functional categories (Fig. 3B; Fig. S7). Over time, transcriptional profiles shifted toward a negative association with PC1 and PC2 for all except the dispersant-only treatments, potentially indicating systematic transcriptional changes associated with either the transition from an open-water system to a microcosm setting or the influence of unique perturbations of the dispersant-only treatment.

Forty-seven DE genes associated with viruses or prophages were identified in the transcriptomic data set, ranging from 8 (WAF treatment) to 17 (CEWAFN) genes per treatment (Fig. 5; Supplemental Data 1). Over half of them were assigned to megaviruses or jumbo phages, while the rest covered cyanobacteria-host viruses (12.8%), *Chrysochromulina ericina* virus (17%), and other viral groups. Most viral DE genes were upregulated (78.7%).

The stress response chaperone protein Hsp70 was consistently upregulated in all the treatments (DISP P value_{adj} = 0.010, WAF P value_{adj} = 0.012, CEWAF P value_{adj} = 0.018, and CEWAFN P value_{adj} = 0.008) and was associated with a *Chrysochromulina ericina* virus or a *Bathycoccus* sp. RCC1105 virus BpV1 (Supplemental Data 1). Similarly, the quinoprotein ethanol dehydrogenase PQQ coding gene was upregulated in all the treatments and was associated with *Pandoravirus inopinatum* or *Pithovirus sibericum*, both classified as megaviruses (16). As expected, genes involved in translation, transcription, and replication, such as GyrA, Rpb1, RpoE, Mg358, and IF3, dominated the upregulation of viral genes for the WAF, dispersant, and CEWAF treatments.

A few viral signatures were exclusively significant for certain species and treatments. An AdoH-AhcY ortholog, similar to SAH hydrolases of potent antiviral activity (17), was exclusively downregulated in the WAF treatment. This result could suggest that dispersants inhibited natural antiviral genes acting in place. Similarly, the major capsid gene P22 associated with the *Alteromonas* phage vB_AmaP_AD45-P1 was only upregulated in the WAF treatment.

DISCUSSION

Detailed analyses of metatranscriptomic data from the Kleindienst et al. (9) microcosm experiment revealed interesting dynamics that were not apparent in the initial assessment. This new information helped elucidate the underlying response modes of the microbial population to differential exposure of oil, dispersant, and nutrients. Dispersant alone was selected for a unique community and for dominant organisms that reflected unique treatment- and time-dependent responses. Similarly, oil alone was selected for a community that was distinct from treatments amended with dispersants. In particular, dispersant- versus oil-amended treatments were selected for different dominant taxa, with *Colwellia* transcripts dominating dispersant treatments and *Marinobacter* transcripts dominating oil-only treatments, mirroring the results of Kleindienst et al. (9). The species-specific responses of these two dominant microorganisms were presented separately (12), but general aspects of their response are discussed here. Dispersant amendment also led to diverging functional profiles among the different treatments. The presence of oil and dispersants with added nutrients led to substantial differences in microbial responses, likely suggesting increased fitness driven by the presence of additional inorganic nutrients. Finally, the oil-only additions led to unanticipated increases in the expression of phages, prophages, transposable elements, and plasmids (PTEPs), suggesting that aspects of microbial community response to oil is driven by the “mobilome” (18), mobile genetic elements in the microbiome.

Dispersants altered expression of key microorganisms: *Colwellia* and *Marinobacter*

Comparison of results from 16S rRNA gene sequencing and metatranscriptomic libraries from the Kleindienst et al. (9) experiment provided insight into the response of microbial

communities to an environmental perturbation, in this case, exposure to different cocktails of organic carbon that were derived from oil and/or dispersant. Based on 16S rDNA gene sequence data, two microorganisms—*Colwellia* and *Marinobacter*—dominated in different treatments: *Colwellia* was more abundant in dispersant-amended treatments, while *Marinobacter* was more abundant in oil-amended treatments. Metatranscriptomics data helped explain the success of these organisms in different experimental treatments (12).

Dispersants increased transcriptomic activity of *Colwellia* spp. (Fig. 1 and 3), in agreement with the original microcosm paper (9) that documented increases in *Colwellia* using 16S rDNA gene sequence data. Similar increases in abundance of *Colwellia* were observed in samples from the DWH ~1,000-m-deep hydrocarbon plume with oil (19), low-molecular-weight dissolved alkanes (20), a Corexit component (i.e., dioctyl sodium sulfosuccinate) (21), and other hydrocarbons with dispersant regimes (22, 23).

Colwellia is a psychrophile with substantial metabolic flexibility (24, 25). Genomic data illustrates a broad metabolic potential for *Colwellia* since its genome encodes the capacity for fermentation (propionate catabolism), beta-oxidation of fatty acids, glycolysis, the tricarboxylic acid cycle, and the pentose phosphate cycle (24). Previous studies have shown that *Colwellia* easily metabolizes glucose, acetate, and lactate (25). Furthermore, *Colwellia* may play a role in ethane and propane cycling (22). *Colwellia* produces polyhydroxyalkanoates as carbon and energy reserves, potentially accounting for the documented upregulation of these compounds in dispersant-amended treatments (Fig. 3B). *Colwellia* is particularly well-suited for polyhydroxyalkanoate production (26). The *Colwellia psychrerythraea* genome (24) contains a diverse suite of genes involved in polyhydroxyalkanoate metabolism, including several that lack homologs in other lineages. Though *Colwellia* spp. have not been shown to oxidize oil- or dispersant-derived organic compounds, genomic data suggest that these microbes could play important roles either in primary or secondary oxidation of oil- and dispersant-derived organic matter (24).

Marinobacter is one of the most common genera found in the global ocean and, as such, plays an important role in pelagic biogeochemical cycles (27). *Marinobacter* exploits environmental niches and survives, even thrives, under various conditions (27, 28). *Marinobacter* is known to oxidize saturated hydrocarbons (alkanes), cycloalkanes, and aromatics (toluene and polycyclic aromatic hydrocarbons) through coupling to aerobic or anaerobic (nitrate reduction) respiration. Unlike *Colwellia*, *Marinobacter* is not a psychrophile; quite the opposite, it is able to thrive in surface and deep waters, deep-sea sediments, and beach sands.

The addition of dissolved oil as a WAF without dispersants stimulated *Marinobacter*'s transcriptomic signals (Fig. 1 and 3). In contrast to *Colwellia*, dispersants limited the growth and replication of *Marinobacter* (9) and also muted their transcriptional activity. The stimulation of *Marinobacter*'s growth in oil-exposed microcosms, in the absence of dispersants, is consistent with reports of *Marinobacter* thriving in oil-rich marine snow flocs generated in the laboratory (29) and in pyrosequencing surveys of *in situ* seawater samples impacted by the DWH oil spill (30, 31). The transcriptomic data suggest that the reduction in *Marinobacter* abundance and activity (9) was not due to competition with *Colwellia* but rather a function of reduced activity, as evidenced by the reduction of transcriptional signal in dispersant treatments. This pattern suggests that dispersants inhibited the metabolic activity of the cosmopolitan oil degrader, *Marinobacter*, reducing its role in oil degradation in treatments amended with dispersants.

Chemical exposure led to rapidly diverging functional profiles

Analyzing the metatranscriptomic data from the Kleindienst et al. (9) experiment also revealed the ecophysiological responses of all microbial groups. The LRD ratio assesses ecophysiological activity where a higher relative cell synthetic capacity, e.g., higher transcription read counts (RNA) relative to DNA, correlates with growth and nutritional status (32, 33). The underlying assumption of the LRD is that the amount of DNA in a

system is stable under changing environmental conditions, while the amount of RNA is altered in response to changing conditions. Generally speaking, organisms thriving under a certain set of conditions will have a higher LRD ratio, while organisms poorly adapted to a given set of conditions will have a lower LRD ratio.

The LRD Group I, with a mean LRD of >3.5 , likely contained highly active microorganisms given the extreme enrichment of transcription read counts over 16S rRNA gene read counts (Fig. 2). Methylophages (i.e., *Methylophaga* and *Methylobacter*) and native hydrocarbon degraders (i.e., *Bermanella* and *Parvibaculum*) were affiliated with this group (15, 34), consistent with previous reports of active indigenous oil degraders including members of these genera (35). *Methylophaga* was also stimulated by the by-products of high-molecular-weight dissolved organic matter metabolism in seawater, suggesting that they are important components of aerobic microbial associations that play key roles in organic carbon turnover (36).

To the best of our knowledge, this is the first report of transcriptional enrichment of *Kordia* in response to dispersants (Fig. 1). Previous studies reported ecological succession of bacterial clades with *Flavobacteriaceae* and *Paracoccaceae* in late August and September 2010 (37, 38). *Kordia*, a member of the *Flavobacteriaceae* family, was recently described at the pangenomic level (39), revealing that its core pangenome comprised a large fraction of cell wall and membrane biogenesis genes, peptidase, and TBDR encoding genes. At t_4 in the dispersant-only treatment, *Kordia* increased transcriptional activity of TBDR, glyoxylate shunt, membrane biogenesis, and peptidase biosynthesis (Fig. 3B and 4; Fig. S4), matching previous descriptions of *Kordia* as an active player in niche colonization (39). Interestingly, the role of *Kordia* in the dispersant treatment was not apparent from the 16S rDNA gene sequence data. Clearly, the role of *Kordia* in dispersant degradation warrants further exploration.

LRD Group II contained taxa with the largest contribution to the microbial transcriptomic profile, underscoring its effective and rapid response to the different chemical cocktails. This group included indigenous hydrocarbon degraders *Oceanospirillales*, *Colwellia*, and *Marinobacter* (Fig. 2), as well as several other known oil degraders, e.g., *Alcanivorax*, a slow-growing *n*-alkane degrading member of the *Gammaproteobacteria* (40), and *Polaribacter*, a member of the *Flavobacteria*, known to degrade polysaccharides (41) as well as hydrocarbons (7). The LRD Group II also included various members of the *Flavobacteriaceae*, the largest family in the phylum *Bacteroidota*, with members capable of aerobic and microaerophilic degradations of polysaccharides and members of the *Alphaproteobacteria*, a class of bacteria in the phylum *Pseudomonadota*.

Members of LRD Group III were poorly adapted for the experimental conditions relative to members of LRD Group I and LRD Group II. LRD Group III included members of the family *Oceanospirillaceae*, such as *Amphritea*, *Pseudospirillum*, and *Balneatrix*, some hydrocarbon degraders, including *Oleiphilus*, *Porticoccus*, *Cycloclasticus*, *Paracoccaceae*, *Rhodobiaceae*, and *Alteromonadaceae*, and members of *Flavobacteria*, *Bacteroidota*, *Pseudobdellovibrionaceae*, and *Spongibacter* (Fig. 2). Many hydrocarbon degraders are slow growing in nature, and membership in LRD Group III could reflect time-sensitive, adaptive responses that occur across different groups of hydrocarbon-degrading bacteria over longer time scales. This pattern may also reflect specific niche-adaptation strategies in hydrocarbon-degrading microbial communities.

From metabolic variations across treatments to viral-phage DE genes

The strongest transcriptomic signals were observed in the “secondary metabolism,” “miscellaneous,” “motility and chemotaxis,” “dormancy and sporulation,” and “RNA metabolism” categories (Fig. 4). The expression trends observed over time usually showed either an expression peak near t_1 for the CEWAF treatment or toward t_4 for the dispersant treatment. The unique trajectories observed in the expression profiles across treatments suggest strongly that different cocktails of complex organic carbon led to distinct time-dependent responses of the microbial populations. These results are consistent with significant shifts observed in the differentially expressed meta

(DEM)-pangenome of *Colwellia* and *Marinobacter* (12), as well as the clustering transitions of taxonomic and functional profiles in the microbial community (Fig. 3)

Pyrrrolnitrin is a secondary metabolite derived from tryptophan and was first isolated from *Pseudomonas pyrocinia*. It is described as a broad-spectrum antifungal and antibacterial agent with application in the control of soilborne pathogens and postharvest diseases, including *Rhizoctonia solani* and *Botrytis cinerea* (42). Pyrrrolnitrin and other halometabolites have been isolated from marine microorganisms, including pentabromopseudilin, found in *Pseudomonas bromoutilis* (43), and bromopyrroles, found in *Pseudoaltermonas* spp. (44). Although pyrrrolnitrin has been widely used to treat human infections, including the fungicide fludioxonil (45), its biosynthesis pathway is still not fully understood. Finding the association of the expression of RebH and PrnA coding sequences with *Pelagibacter* phages, cyanobacteria-host phages, and *Colwellia* sp. MT41 suggests a new mechanism that potentially improves the ecological fitness of *Colwellia* and phage-controlled microbes to dispersant-polluted environments. We hypothesize two possible explanations:

1. The biosynthesis of intermediates with bacteriocide activity. The reaction kinetics of flavin-dependent tryptophan halogenase requires first the completion of flavin redox reactions followed by substrate chlorination (46, 47), leading to the formation of harmful reactive species such as hypochlorite and peroxide.
2. A still unknown flavin-dependent tryptophan halogenase may be participating in the redox modulation of virus-host receptor interactions. Pathway coordination aiming for redox balance has been associated with the successful reactivation of viral infectivity through stable receptor recognition. This phenomenon has been described previously, including virus-host receptor interactions of human diseases such as severe acute respiratory syndrome coronavirus 2 and HIV (48, 49).

Both hypotheses remain open to further investigation.

To inspect expression changes in PTEPs, we selected gene counts associated with phages or viruses after performing DE analysis to the complete data set. The megaviruses and jumbo phages were the only functional group with the highest relative peak in the oil-only treatment (Fig. S4). Further inspection of DE genes assigned to viral groups revealed that most viral DE genes were upregulated in all of the amended treatments, while downregulation was observed only in the CEWAFN treatment (Fig. 5).

Megaviruses are important, yet poorly understood, components of ocean ecosystems (16, 18, 50, 51). Megaviruses can infect the ciliate and flagellate grazers that impart top-down control on microbial populations (52, 53). As such, an intriguing possibility is that the ingrowth of megaviruses in response to oil exposure could relax predation and allow populations of oil degraders to bloom in the absence of predators. Megaviruses may serve a key role in the case of oil spills and the microbial response to them, i.e., the presence of megaviruses may promote the success of oil-degrading microbial communities directly (54). Genomic comparisons of megaviruses isolated in coastal waters revealed the paradox of megaviruses showing convergent evolution, while the number of unique protein-coding genes overwhelmingly outnumbered their core genes (55). Hence, this is an open opportunity to identify the role of the adaptive pangenome of megaviruses through the lens of a metatranscriptomic data set. Additional work is under way to create a megavirus DEM-pangenome following the procedure in Peña-Montenegro et al. (12, 56).

The viral repertoire was different in the CEWAF versus the CEWAFN treatment. The inherent stress imposed on the microbial community through nutrient limitation appears to have led to a more substantial viral-induced stress response in the CEWAF treatment compared to the CEWAFN treatment (Fig. 5). These results could be associated with changes in the microbial activity and the formation of marine oil snow patterns reported by Kleindienst et al. (9), as well as perturbations at the expression level, including lipid metabolism and hydrocarbon degradation genes, in *Colwellia* (12). Such positive stimulation for degradation and stress response activities under nutrient amendment

could be indicative of an underlying nutrient-limited system, as suggested elsewhere (57). Previous studies showed how environmental conditions impacted the relationship between viruses and bacteria using multivariate models demonstrating that environmental factors, such as inorganic nutrient concentrations, are important predictors of host and viral abundance across a broad range of temporal and spatial scales (58). Similarly, trophic interactions in the microbial food web, such as predation and the availability of limiting nutrients, were shown to affect the structure and function of viral and prokaryote communities (59). We suspect that the absence of nutrients, i.e., nutrient limitation, could have triggered stress responses in the microbial communities, with a collateral effect on the activation of viral communities.

Conclusions

Comparison of results from 16S rRNA gene sequencing and metatranscriptomic libraries from the Kleindienst et al. (9) experiment provided insight into the response of microbial communities to an environmental perturbation, in this case, exposure to differential cocktails of organic carbon that were derived from oil and/or dispersant. The presence of dispersant increased transcriptomic activity of *Colwellia* spp., and *Colwellia* may have been involved in the degradation of oil or dispersant components in the microcosms, as well as in field samples (22, 23). In contrast, dispersants limited the growth and replication of *Marinobacter* (9) and also muted their transcriptional activity, reducing its role in oil degradation in treatments amended with dispersants. The LRD ratio proved to be a valid tool to assess microbial groups' relative ecophysiological activity levels across treatments and in response to nutritional status, showing that some oil-degrading microorganisms are more adept at responding to oil or oil plus dispersant exposure than others. Transcriptional data revealed a potentially important role for *Kordia* in the metabolism of dispersant-derived organic matter; the importance of these organisms was not clear from 16S rRNA gene composition data. The upregulation of genes from megaviruses, especially in oil-only treatments, suggests an important role for these organisms in shaping the oil-spill-perturbed microbiome. Accelerated activity of megaviruses could relieve grazing pressure on oil-degrading microorganisms, hence promoting their rapid growth in response to oil infusions. The presence of dispersants may inhibit this, which could explain why different microbial populations thrive under conditions of oil versus dispersant exposure.

MATERIALS AND METHODS

Microcosm setup

Methods in this section were described in detail and performed by Kleindienst et al. (9). In brief, deep water was collected at 1,178-m depth in the northern Gulf of Mexico (latitude 27.3614, longitude -90.6018). Water was stored in 20-L carboys and transported to the University of Georgia laboratory. Seventy-two glass bottles (1.8-L sample per bottle) were incubated on a roller table. Each treatment aimed to simulate the DWH deepwater plume. Treatments resulted from the mixture of pasteurized seawater with WAF of oil-only (DWH plume *in situ* dissolved organic carbon ~150 μ M), synthetic DISP Corexit 9500 (~19 μ g/L), and CEWAF (WAF + Corexit 9500 ~ 19 μ g/L). CEWAFN treatment was amended with 10- μ M ammonium chloride, 10- μ M potassium nitrate, 1- μ M potassium phosphate, final concentrations, and trace metals. Sampling was performed over five time points in a span of 6 weeks (t_0 = 0 day, t_1 = 7 days, t_2 = 17 days, t_3 = 28 days, and t_4 = 42 days), except for the CEWAFN treatment only, including t_0 , t_1 , and t_4 . The biotic control was not amended.

Sampling and sequencing

Filters were frozen in liquid nitrogen, kept on dry ice for shipping, and stored in the laboratory at -80°C . RNA was purified from filters using the Trizol reagent (Life Technologies, Carlsbad, CA, USA) and treated with DNase (Qiagen, Valencia, CA, USA). RNA quality was analyzed using a 2100 Bioanalyzer with Agilent RNA 6000 Nano Kits (Agilent Technologies, Santa Clara, CA, USA) and quantified using the Qubit Fluorometric Quantification system (Thermo Fisher, Waltham, MA, USA). Total RNA (10–100 ng) was subjected to amplification and cDNA synthesis using the Ovation RNA-Seq System (version 2) (NuGEN). One microgram of the resulting high-quality cDNA pool was fragmented to a mean length of 200 bp, and Truseq (Illumina) libraries were prepared and subjected to paired-end sequencing via Illumina HiSeq.

Data workflow

Paired-end libraries were imported into FASTQC (<http://www.bioinformatics.bbsrc.ac.uk/projects/fastqc>) to scan for sequencing quality. Adapter removal, read, and quality trimming were completed in Trimmomatic (version 0.36) (60), where a 4-bp sliding window was applied to retain bases with quality scores greater than 20. Trimmed paired-end reads were assembled with Trinity (version r20140717) (61) to generate *de novo* reference transcriptomes (mean contig length: 460 bp, mean N50: 487 bp, mean total: 34 million bp) for each of the samples. We used Prodigal (version 2.6.3) (62) with default settings to identify open reading frames. Reference assembly annotations were determined by BLASTX (version 2.2.31) query searches against the National Center for Biotechnology Information (NCBI) non-redundant protein database, SwissProt, and TrEMBL (63, 64). Gene ontology annotations were determined by mapping SwissProt/TrEMBL IDs to the UniProt-GOA database (65). Viral contigs were confirmed with MetaPhinder (66). To compensate for potential data processing biases of our selected annotation procedure, we included an automatic annotation strategy as follows. Paired-end reads for each library were merged and imported into MG-RAST (version 4.0.3) (67). Taxonomic and functional hits were queried against the MG-RAST Subsystems database ($\leq 1e-4$, $\geq 33\%$ identity, minimum alignment length 15 aa). Annotation calls from BLASTX and MG-RAST were integrated by using the totalannotation.py script found in the De Wit et al. pipeline (68).

Given the complex and variable taxonomic labeling systems across the annotation sources, we developed an R script to (i) translate from variable taxonomic labels into a unified and restricted vocabulary space and (ii) aggregate a large list of taxonomic labels into a smaller list by combining taxonomic calls of low relative abundance into higher-rank taxonomic groups until reaching a minimum relative abundance threshold. This tool is detailed in our dedicated GitHub module (<https://github.com/biotemon/TaxonomyModule>). The input for the script was an array with observations in tuple format (*sample_id*, *query*, and *counts*). Then, the script generated a matrix representation of the query label in terms of the SQLite reference table. If relative *counts* (*r*) for a given *query* representation (*q*) were below a minimum threshold (*T*) (e.g., 4%), the script merged *r* to the next higher taxonomic rank until $r \geq T$.

Differential expression analysis

We aligned all libraries to assembled transcriptomes using Bowtie2 (69). To contrast gene expression with respect to the biotic control, we used HTSeq-count to generate the read counts of genes recruited by the reference genomes (70). Profiles were normalized across all samples using the regularized logarithm transformation as implemented in DESeq2 using a generalized linear model (71). Then, statistical inference was performed using the negative binomial Wald test with Cook's distance to control for outliers (72). Those genes with an adjusted *P* value of < 0.05 (using the Benjamini-Hochberg method) were classified as DE genes (73).

LRD and diversity analysis

To calculate LRD ratios, we used operational taxonomic unit (OTU) abundance counts obtained from the Kleindienst et al. data set (9). Raw 16S rRNA gene amplicon sequences are available under the NCBI Bioproject PRJNA253405. Relative OTU abundance triplicates were averaged (\bar{d}) and subjected to a higher-rank taxonomic merging with a minimum relative abundance threshold of 4%. LRD index is defined as

$$LRD_{ij} = \frac{1}{n} \sum_{t=1}^n \log_2 \frac{r_{ijt}}{d_{ijt}}$$

where the log-fold ratio between metatranscriptomic (r) and 16S rDNA gene (\bar{d}) relative counts are averaged across time (t) for each taxonomic group (i) and treatment (j).

Rarefaction and alpha-diversity analyses of metatranscriptomic data sets were performed through MG-RAST. To evaluate beta-dispersion at the expression level of the microbial communities between all treatments, beta-phylogenetic differences weighted by abundance were tested using comdist (the average MPD for each species in a sample to all species in another sample) and comdistnt (the average MNTD for all species in a sample to the nearest neighbors in another sample) using the package Picante (74). A sequence-based reference phylogenetic tree was used as input parameter for the MPD and MNTD distance matrix calculations. To build the reference phylogenetic tree, we followed procedures described previously (75). In brief, taxonomic representatives shown in Fig. 1 were selected for searches of archaeal, bacterial, and eukaryotic ribosomal small subunit sequences as well as viral capsid and coat protein coding sequences. A full description of taxonomic representative sequences is available in Supplemental Data 2. Sequences were aligned in MAFFT. Maximum likelihood phylogenetic trees of aligned sequences were inferred with RAxML using the general time-reversible model for substitution and the GAMMA model for rate heterogeneity. Tree topologies were checked by 100 bootstrapping replicates.

Bray-Curtis dissimilarity among all treatments was calculated as an abundance-weighted measure of beta-diversity. The output distance matrix was visualized via PCA ordinations using the pcoa function from the ape package. The function adonis from the vegan package was used to examine the significant relationship between distance matrices (U) (i.e., Bray-Curtis dissimilarity, MPD, or MNTD) and experimental factors: dispersant (D), WAF (O), nutrients (N), and time (t). Each test comprised 999 permutations. The testing model was defined as follows:

$$U = O + D + O \times D + O \times D \times N + t + O \times t + D \times t + O \times D \times t + O \times D \times N \times t$$

ACKNOWLEDGMENTS

This study was funded by the Gulf of Mexico Research Initiative grant “Ecosystem Impacts of Oil and Gas Inputs to the Gulf.” We thank the Schmidt Ocean Institute for providing time at sea in the Gulf of Mexico on the *RV Falkor* (cruise FK06a). This study was also supported in part by resources and technical expertise from the Georgia Advances Computing Resource Center, a partnership between the University of Georgia’s Office of the Provost, the Office of the Vice President for Research, and the Office of the Vice President for Information Technology. T.D.P.-M. was supported partially by a Fulbright Colombia fellowship.

We thank Kimberley S. Hunter for assistance with laboratory measurements.

AUTHOR AFFILIATIONS

¹Department of Marine Sciences, University of Georgia, Athens, Georgia, USA

²Institute of Bioinformatics, University of Georgia, Athens, Georgia, USA

³Grupo de Investigación y Desarrollo en Ciencias, Tecnología e Innovación (BioGRID), Sociedad de Doctores e Investigadores de Colombia (SoPhIC), Bogotá, Colombia

⁴Microbial and Environmental Genomics, J. Craig Venter Institute, La Jolla, California, USA

⁵Integrative Oceanography Division, Scripps Institution of Oceanography, UC San Diego, La Jolla, California, USA

⁶Department of Medicine, University of Chicago, Chicago, Illinois, USA

⁷Josephine Bay Paul Center, Marine Biological Laboratory, Woods Hole, Massachusetts, USA

⁸Department of Genetics, University of Georgia, Athens, Georgia, USA

PRESENT ADDRESS

Sara Kleindienst, Department of Environmental Microbiology, Institute for Sanitary Engineering, Water Quality and Solid Waste Management (ISWA), University of Stuttgart, Stuttgart, Germany

AUTHOR ORCIDs

Tito D. Peña-Montenegro  <http://orcid.org/0000-0002-2646-4183>

A. Murat Eren  <http://orcid.org/0000-0001-9013-4827>

Samantha B. Joye  <http://orcid.org/0000-0003-1610-451X>

FUNDING

Funder	Grant(s)	Author(s)
Gulf of Mexico Research Initiative (GoMRI)	ECOGIG	Tito D. Peña-Montenegro Sara Kleindienst Andrew E. Allen A. Murat Eren John P. McCrow Jonathan Arnold Samantha B. Joye

AUTHOR CONTRIBUTIONS

Tito D. Peña-Montenegro, Data curation, Methodology, Software, Writing – original draft, Writing – review and editing | Sara Kleindienst, Conceptualization, Investigation, Writing – review and editing | Andrew E. Allen, Data curation, Investigation, Methodology, Writing – review and editing | A. Murat Eren, Formal analysis, Methodology, Resources, Software, Writing – review and editing | John P. McCrow, Data curation, Investigation | Jonathan Arnold, Formal analysis, Methodology, Supervision, Writing – review and editing | Samantha B. Joye, Conceptualization, Formal analysis, Funding acquisition, Investigation, Methodology, Project administration, Resources, Supervision, Writing – original draft, Writing – review and editing

DATA AVAILABILITY

Raw sequencing reads generated for this study can be found in the Sequence Read Archive under BioProject [PRJNA640753](#). MG-RAST annotation output is publicly available at <https://www.mg-rast.org/linkin.cgi?project=mgp84528>. All scripts are found on GitHub (<https://github.com/biotemon/K2015> and <https://github.com/biotemon/TaxonomyModule>). Taxonomy rank database and all other data are available in the Open Science Framework repository at <https://osf.io/fu9bw/>.

ADDITIONAL FILES

The following material is available [online](#).

Supplemental Material

SuppCode_1 (AEM01083-24-s0001.pdf). Supplemental code part 1.

SuppCode_2 (AEM01083-24-s0002.pdf). Supplemental code part 2.

SuppData1 (AEM01083-24-s0003.xlsx). Differential expression analysis and annotation of predicted gene sequences in the Kleindienst et al. metatranscriptome.

SuppData2 (AEM01083-24-s0004.xlsx). Representative sequences to build a guiding phylogenetic tree for phylobetadiversity analysis of the metatranscriptomic dataset.

Supplemental figures (AEM01083-24-s0005.pdf). Figures S1 to S7.

REFERENCES

- Joye S, Kostka JE. 2020. Microbial genomics of the global ocean system: report on an American Academy of Microbiology (Academy), the American Geophysical Union (AGU), and the Gulf of Mexico Research Initiative (GoMRI) colloquium held on 9 and 10 April 2019. American Society for Microbiology.
- Harrison S. 2017. Lessons from the Taylor Energy oil spill: history, seasonality, and nutrient limitation. University of Georgia, Athens, GA, USA.
- National Academies Press. 2003. Committee on oil in the sea: inputs, fates, and effects, ocean studies board, marine board, transportation research board, division on earth and life studies. Oil in the Sea III: Inputs, Fates, and Effects. National Academies Press, Washington, D.C. Available from: <https://www.nap.edu/catalog/10388>. Retrieved 22 Mar 2021.
- Committee on the Evaluation of the Use of Chemical Dispersants in Oil Spill Response, Ocean Studies Board, Board on Environmental Studies and Toxicology, Division on Earth and Life Studies, National Academies of Sciences, Engineering, and Medicine. 2020. The use of Dispersants in Marine oil spill response. National Academies Press, Washington, D.C. Available from: <https://www.nap.edu/catalog/25161>. Retrieved 22 Mar 2021.
- Place BJ, Perkins MJ, Sinclair E, Barsamian AL, Blakemore PR, Field JA. 2016. Trace analysis of surfactants in Corexit oil dispersant formulations and seawater. *Deep Sea Res II Top Stud Oceanogr* 129:273–281. <https://doi.org/10.1016/j.dsr2.2014.01.015>
- Baelum J, Borglin S, Chakraborty R, Fortney JL, Lamendella R, Mason OU, Auer M, Zemla M, Bill M, Conrad ME, Malfatti SA, Tringe SG, Holman H-Y, Hazen TC, Jansson JK. 2012. Deep-sea bacteria enriched by oil and dispersant from the Deepwater Horizon spill: enrichment of oil degraders from Gulf of Mexico. *Environ Microbiol* 14:2405–2416.
- Brakstad OG, Throne-Holst M, Netzer R, Stoeckel DM, Atlas RM. 2015. Microbial communities related to biodegradation of dispersed Macondo oil at low seawater temperature with Norwegian coastal seawater: microbial communities during oil biodegradation. *Microb Biotechnol* 8:989–998. <https://doi.org/10.1111/1751-7915.12303>
- Kleindienst S, Grim S, Sogin M, Bracco A, Crespo-Medina M, Joye SB. 2016. Diverse, rare microbial taxa responded to the deepwater horizon deep-sea hydrocarbon plume. *ISME J* 10:400–415. <https://doi.org/10.1038/ismej.2015.121>
- Kleindienst S, Seidel M, Ziervogel K, Grim S, Loftis K, Harrison S, Malkin SY, Perkins MJ, Field J, Sogin ML, Dittmar T, Passow U, Medeiros PM, Joye SB. 2015. Chemical dispersants can suppress the activity of natural oil-degrading microorganisms. *Proc Natl Acad Sci U S A* 112:14900–14905. <https://doi.org/10.1073/pnas.1507380112>
- Seidel M, Kleindienst S, Dittmar T, Joye SB, Medeiros PM. 2016. Biodegradation of crude oil and dispersants in deep seawater from the Gulf of Mexico: insights from ultra-high resolution mass spectrometry. *Deep Sea Res Part II: Topical Stud Oceanogr* 129:108–118. <https://doi.org/10.1016/j.dsr2.2015.05.012>
- Ziervogel K, Joye SB, Kleindienst S, Malkin SY, Passow U, Steen AD, Arnosti C. 2019. Polysaccharide hydrolysis in the presence of oil and dispersants: insights into potential degradation pathways of exopolymeric substances (EPS) from oil-degrading bacteria. *Elementa* 7:31. <https://doi.org/10.1525/elementa.371>
- Peña-Montenegro TD, Kleindienst S, Allen AE, Eren AM, McCrow JP, Sánchez-Calderón JD, Arnold J, Joye SB. 2023. Species-specific responses of marine bacteria to environmental perturbation. *ISME COMMUN* 3:99. <https://doi.org/10.1038/s43705-023-00310-z>
- Chakraborty R, Borglin SE, Dubinsky EA, Andersen GL, Hazen TC. 2012. Microbial response to the MC-252 oil and Corexit 9500 in the Gulf of Mexico. *Front Microbiol* 3:357. <https://doi.org/10.3389/fmicb.2012.00357>
- Coate JE, Doyle JJ. 2015. Variation in transcriptome size: are we getting the message? *Chromosoma* 124:27–43. <https://doi.org/10.1007/s00412-014-0496-3>
- Schleheck D, Weiss M, Pitluck S, Bruce D, Land ML, Han S, Saunders E, Tapia R, Detter C, Brettin T, Han J, Woyke T, Goodwin L, Pennacchio L, Nolan M, Cook AM, Kjelleberg S, Thomas T. 2011. Complete genome sequence of *Parvibaculum lavamentivorans* type strain DS-1T. *Stand Genomic Sci* 5:298–310. <https://doi.org/10.4056/signs.2215005>
- Legendre M, Fabre E, Poirot O, Jeudy S, Lartigue A, Alempic J-M, Beucher L, Philippe N, Bertaux L, Christo-Foroux E, Labadie K, Couté Y, Abergel C, Claverie J-M. 2018. Diversity and evolution of the emerging pandoraviridae family. *Nat Commun* 9:2285. <https://doi.org/10.1038/s41467-018-04698-4>
- De Clercq E. 2005. John montgomery's legacy: carbocyclic adenosine analogues as SAH hydrolase inhibitors with broad-spectrum antiviral activity. *Nucleos Nucleic Acids* 24:1395–1415. <https://doi.org/10.1080/15257770500265638>
- Carr VR, Shkoporov A, Hill C, Mullany P, Moyes DL. 2021. Probing the mobilome: discoveries in the dynamic microbiome. *Trends Microbiol* 29:158–170. <https://doi.org/10.1016/j.tim.2020.05.003>
- Wade TL, Sweet ST, Sericano JL, Guinasso NL, Diercks A-R, Highsmith RC, Asper VL, Joung D, Shiller AM, Lohrenz SE, Joye SB. 2011. Analyses of water samples from the deepwater horizon oil spill: documentation of the subsurface plume, p 77–82. In Liu Y, MacFadyen A, Ji ZG, Weisberg RH (ed), *Geophysical monograph series*. American Geophysical Union, Washington, D. C.
- Joye SB, MacDonald IR, Leifer I, Asper V. 2011. Magnitude and oxidation potential of hydrocarbon gases released from the BP oil well blowout. *Nature Geosci* 4:160–164. <https://doi.org/10.1038/ngeo1067>
- Kujawinski EB, Kido Soule MC, Valentine DL, Boysen AK, Longnecker K, Redmond MC. 2011. Fate of Dispersants associated with the deepwater horizon oil spill. *Environ Sci Technol* 45:1298–1306. <https://doi.org/10.1021/es103838p>
- Redmond MC, Valentine DL. 2012. Natural gas and temperature structured a microbial community response to the deepwater horizon oil spill. *Proc Natl Acad Sci U S A* 109:20292–20297. <https://doi.org/10.1073/pnas.1108756108>
- Mason OU, Han J, Woyke T, Jansson JK. 2014. Single-cell genomics reveals features of a *Colwellia* species that was dominant during the deepwater horizon oil spill. *Front Microbiol* 5:332. <https://doi.org/10.3389/fmicb.2014.00332>
- Méthé BA, Nelson KE, Deming JW, Momen B, Melamud E, Zhang X, Moulton J, Madupu R, Nelson WC, Dodson RJ, et al. 2005. The psychrophilic

- lifestyle as revealed by the genome sequence of *Colwellia psychrerythraea* 34H through genomic and proteomic analyses. *Proc Natl Acad Sci U S A* 102:10913–10918. <https://doi.org/10.1073/pnas.0504766102>
25. Czajka JJ, Abernathy MH, Benites VT, Baidoo EEK, Deming JW, Tang YJ. 2018. Model metabolic strategy for heterotrophic bacteria in the cold ocean based on *Colwellia psychrerythraea* 34H. *Proc Natl Acad Sci U S A* 115:12507–12512. <https://doi.org/10.1073/pnas.1807804115>
 26. Crisafi F, Valentino F, Micolucci F, Denaro R. 2022. From organic wastes and hydrocarbons pollutants to polyhydroxyalkanoates: bioconversion by terrestrial and marine bacteria. *Sustainability* 14:8241. <https://doi.org/10.3390/su14148241>
 27. Singer E, Webb EA, Nelson WC, Heidelberg JF, Ivanova N, Pati A, Edwards KJ. 2011. Genomic potential of *Marinobacter aquaeolei*, a biogeochemical “opportunistic”. *Appl Environ Microbiol* 77:2763–2771. <https://doi.org/10.1128/AEM.01866-10>
 28. Pinto J, Lami R, Krasovec M, Grimaud R, Urios L, Lupette J, Escande M-L, Sanchez F, Intertaglia L, Grimsley N, Piganeau G, Sanchez-Brosseau S. 2021. Features of the opportunistic behaviour of the marine bacterium *Marinobacter algicola* in the microalga *Ostreococcus tauri* phycosphere. *Microorganisms* 9:1777. <https://doi.org/10.3390/microorganisms9081777>
 29. McKay LJ, Gutierrez T, Teske AP. 2016. Development of a group-specific 16S rRNA-targeted probe set for the identification of *Marinobacter* by fluorescence in situ hybridization. *Deep Sea Res Part II: Topical Stud Ocean* 129:360–367. <https://doi.org/10.1016/j.dsr2.2013.10.009>
 30. Gutierrez T, Singleton DR, Berry D, Yang T, Aitken MD, Teske A. 2013. Hydrocarbon-degrading bacteria enriched by the deepwater horizon oil spill identified by cultivation and DNA-SIP. *ISME J* 7:2091–2104. <https://doi.org/10.1038/ismej.2013.98>
 31. Yang T, Nigro LM, Gutierrez T, D’Ambrosio L, Joye SB, Highsmith R, Teske A. 2016. Pulsed blooms and persistent oil-degrading bacterial populations in the water column during and after the deepwater horizon blowout. *Deep Sea Res Part II: Topical Stud Ocean* 129:282–291. <https://doi.org/10.1016/j.dsr2.2014.01.014>
 32. Dlott G, Maul JE, Buyer J, Yarwood S. 2015. Microbial rRNA:RDNA gene ratios may be unexpectedly low due to extracellular DNA preservation in soils. *J Microbiol Methods* 115:112–120. <https://doi.org/10.1016/j.mimet.2015.05.027>
 33. Chicharo MA, Chicharo L. 2008. RNA:DNA ratio and other nucleic acid derived indices in marine ecology. *Int J Mol Sci* 9:1453–1471. <https://doi.org/10.3390/ijms9081453>
 34. King GM, Kostka JE, Hazen TC, Sobecky PA. 2015. Microbial responses to the deepwater horizon oil spill: from Coastal wetlands to the deep sea. *Ann Rev Mar Sci* 7:377–401. <https://doi.org/10.1146/annurev-marine-010814-015543>
 35. Chen Q, Bao B, Li Y, Liu M, Zhu B, Mu J, Chen Z. 2020. Effects of marine oil pollution on microbial diversity in coastal waters and stimulating indigenous microorganism Bioremediation with nutrients. *Reg Stud Marine Sci* 39:101395. <https://doi.org/10.1016/j.rsma.2020.101395>
 36. McCarren J, Becker JW, Repeta DJ, Shi Y, Young CR, Malmstrom RR, Chisholm SW, DeLong EF. 2010. Microbial community transcriptomes reveal microbes and metabolic pathways associated with dissolved organic matter turnover in the sea. *Proc Natl Acad Sci U S A* 107:16420–16427. <https://doi.org/10.1073/pnas.1010732107>
 37. Dubinsky EA, Conrad ME, Chakraborty R, Bill M, Borglin SE, Hollibaugh JT, Mason OU, M. Piceno Y, Reid FC, Stringfellow WT, Tom LM, Hazen TC, Andersen GL. 2013. Succession of hydrocarbon-degrading bacteria in the aftermath of the deepwater horizon oil spill in the Gulf of Mexico. *Environ Sci Technol* 47:10860–10867. <https://doi.org/10.1021/es401676y>
 38. Hazen TC, Dubinsky EA, DeSantis TZ, Andersen GL, Piceno YM, Singh N, Jansson JK, Probst A, Borglin SE, Fortney JL, et al. 2010. Deep-sea oil plume enriches indigenous oil-degrading bacteria. *Science* 330:204–208. <https://doi.org/10.1126/science.1195979>
 39. Royo-Llonch M, Sánchez P, González JM, Pedrós-Alió C, Acinas SG. 2020. Ecological and functional capabilities of an uncultured *Kordia* SP. *Syst Appl Microbiol* 43:126045. <https://doi.org/10.1016/j.syapm.2019.126045>
 40. Schneider S, dos Santos VAM, Bartels D, Bekel T, Brecht M, Buhmester J, Chernikova TN, Denaro R, Ferrer M, Gertler C, et al. 2006. Genome sequence of the ubiquitous hydrocarbon-degrading marine bacterium *Alcanivorax borkumensis*. *Nat Biotechnol* 24:997–1004. <https://doi.org/10.1038/nbt1232>
 41. Xing P, Hahnke RL, Unfried F, Markert S, Huang S, Barbeyron T, Harder J, Becher D, Schweder T, Glöckner FO, Amann RI, Teeling H. 2015. Niches of two polysaccharide-degrading *Polaribacter* isolates from the North Sea during a spring Diatom bloom. *ISME J* 9:1410–1422. <https://doi.org/10.1038/ismej.2014.225>
 42. Zhang J, Mavrodi DV, Yang M, Thomashow LS, Mavrodi OV, Kelton J, Weller DM. 2020. *Pseudomonas synxantha* 2-79 transformed with pyrrolnitrin biosynthesis genes has improved biocontrol activity against soilborne pathogens of wheat and canola. *Phytopathology* 110:1010–1017. <https://doi.org/10.1094/PHYTO-09-19-0367-R>
 43. Burkholder PR, Pfister RM, Leitz FH. 1966. Production of a Pyrrole antibiotic by a Marine bacterium. *Appl Microbiol* 14:649–653. <https://doi.org/10.1128/am.14.4.649-653.1966>
 44. Agarwal V, El Gamal AA, Yamanaka K, Poth D, Kersten RD, Schorn M, Allen EE, Moore BS. 2014. Biosynthesis of polybrominated aromatic organic compounds by marine bacteria. *Nat Chem Biol* 10:640–647. <https://doi.org/10.1038/nchembio.1564>
 45. Brandhorst TT, Kean IRL, Lawry SM, Wiesner DL, Klein BS. 2019. Phenylpyrrole fungicides act on Triosephosphate isomerase to induce methylglyoxal stress and alter hybrid histidine kinase activity. *Sci Rep* 9:5047. <https://doi.org/10.1038/s41598-019-41564-9>
 46. Yeh E, Cole LJ, Barr EW, Bollinger JM, Ballou DP, Walsh CT. 2006. Flavin redox chemistry precedes substrate chlorination during the reaction of the Flavin-dependent Halogenase Rebh. *Biochemistry* 45:7904–7912. <https://doi.org/10.1021/bi060607d>
 47. Dong C, Flecks S, Unversucht S, Haupt C, van Pée K-H, Naismith JH. 2005. Tryptophan 7-halogenase (PnA) structure suggests a mechanism for regioselective chlorination. *Science* 309:2216–2219. <https://doi.org/10.1126/science.1116510>
 48. Singh S, Ghosh S, Pal VK, Munshi M, Shekar P, Narasimha Murthy DT, Mughesh G, Singh A. 2021. Antioxidant nanozyme counteracts HIV - 1 by modulating intracellular redox potential. *EMBO Mol Med* 13:e13314. <https://doi.org/10.15252/emmm.202013314>
 49. Singh J, Dhindsa RS, Misra V, Singh B. 2020. SARS-CoV2 infectivity is potentially modulated by host redox status. *Comput Struct Biotechnol J* 18:3705–3711. <https://doi.org/10.1016/j.csbj.2020.11.016>
 50. Arslan D, Legendre M, Seltzer V, Abergel C, Claverie J-M. 2011. Distant mimivirus relative with a larger genome highlights the fundamental features of megaviridae. *Proc Natl Acad Sci U S A* 108:17486–17491. <https://doi.org/10.1073/pnas.1110889108>
 51. Tokarz-Deptuła B, Niedźwiedzka-Rystwej P, Czupryńska P, Deptuła W. 2019. Protozoal giant viruses: agents potentially infectious to humans and animals. *Virus Genes* 55:574–591. <https://doi.org/10.1007/s11262-019-01684-w>
 52. Talmy D, Beckett SJ, Zhang AB, Taniguchi DAA, Weitz JS, Follows MJ. 2019. Contrasting controls on microzooplankton grazing and viral infection of microbial prey. *Front Mar Sci* 6:182. <https://doi.org/10.3389/fmars.2019.00182>
 53. Chow C-E, Kim DY, Sachdeva R, Caron DA, Fuhrman JA. 2014. Top-down controls on bacterial community structure: microbial network analysis of bacteria, T4-like viruses and protists. *ISME J* 8:816–829. <https://doi.org/10.1038/ismej.2013.199>
 54. Breitbart M, Bonnain C, Malki K, Sawaya NA. 2018. Phage puppet masters of the marine microbial realm. *Nat Microbiol* 3:754–766. <https://doi.org/10.1038/s41564-018-0166-y>
 55. Gallot-Lavallée L, Blanc G, Claverie J-M. 2017. Comparative genomics of *Chrysochromulina ericina* virus and other microalga-infecting large DNA viruses highlights their intricate evolutionary relationship with the established mimiviridae family. *J Virol* 91:e00230-17. <https://doi.org/10.1128/JVI.00230-17>
 56. Peña-Montenegro TD, Kleindienst S, Allen AE, Eren AM, McCrow JP, Sánchez-Calderón JD, Arnold J, Joye SB. 2020. *Colwellia* and *Marinobacter* metapangenomes reveal species-specific responses to oil and dispersant exposure in deepsea microbial communities. *Microbiology*. <https://doi.org/10.1101/2020.09.28.317438>
 57. Shiller AM, Joung D. 2012. Nutrient depletion as a proxy for microbial growth in deepwater horizon subsurface oil/gas plumes. *Environ. Res. Lett* 7:045301. <https://doi.org/10.1088/1748-9326/7/4/045301>
 58. Finke JF, Hunt BPV, Winter C, Carmack EC, Suttle CA. 2017. Nutrients and other environmental factors influence virus abundances across oxic and

- hypoxic marine environments. *Viruses* 9:152. <https://doi.org/10.3390/v9060152>
59. Sandaa R-A, Pree B, Larsen A, Våge S, Tøpper B, Tøpper JP, Thyraug R, Thingstad TF. 2017. The response of heterotrophic prokaryote and viral communities to labile organic carbon inputs is controlled by the predator food chain structure. *Viruses* 9:238. <https://doi.org/10.3390/v9090238>
60. Bolger AM, Lohse M, Usadel B. 2014. Trimmomatic: a flexible trimmer for Illumina sequence data. *Bioinformatics* 30:2114–2120. <https://doi.org/10.1093/bioinformatics/btu170>
61. Haas BJ, Papanicolaou A, Yassour M, Grabherr M, Blood PD, Bowden J, Couger MB, Eccles D, Li B, Lieber M, MacManes MD, Ott M, Orvis J, Pochet N, Strozzi F, Weeks N, Westerman R, William T, Dewey CN, Henschel R, LeDuc RD, Friedman N, Regev A. 2013. *De novo* transcript sequence reconstruction from RNA-seq using the trinity platform for reference generation and analysis. *Nat Protoc* 8:1494–1512. <https://doi.org/10.1038/nprot.2013.084>
62. Hyatt D, Chen G-L, Locascio PF, Land ML, Larimer FW, Hauser LJ. 2010. Prodigal: prokaryotic gene recognition and translation initiation site identification. *BMC Bioinformatics* 11:1–11. <https://doi.org/10.1186/1471-2105-11-119>
63. Boeckmann B, Bairoch A, Apweiler R, Blatter M-C, Estreicher A, Gasteiger E, Martin MJ, Michoud K, O'Donovan C, Phan I, Pilbout S, Schneider M. 2003. The SWISS-PROT protein knowledgebase and its supplement TrEMBL in 2003. *Nucleic Acids Res* 31:365–370. <https://doi.org/10.1093/nar/gkg095>
64. Altschul SF, Gish W, Miller W, Myers EW, Lipman DJ. 1990. Basic local alignment search tool. *J Mol Biol* 215:403–410. [https://doi.org/10.1016/S0022-2836\(05\)80360-2](https://doi.org/10.1016/S0022-2836(05)80360-2)
65. Dummer EC, Huntley RP, Alam-Faruque Y, Sawford T, O'Donovan C, Martin MJ, Bely B, Browne P, Mun Chan W, Eberhardt R, et al. 2012. The UniProt-GO annotation database in 2011. *Nucleic Acids Res* 40:D565–70. <https://doi.org/10.1093/nar/gkr1048>
66. Jurtz VI, Villarroel J, Lund O, Voldby Larsen M, Nielsen M. 2016. MetaPhinder—identifying bacteriophage sequences in metagenomic data SETS. *PLoS One* 11:e0163111. <https://doi.org/10.1371/journal.pone.0163111>
67. Meyer F, Paarmann D, D'Souza M, Olson R, Glass E, Kubal M, Paczian T, Rodriguez A, Stevens R, Wilke A, Wilkening J, Edwards R. 2008. The metagenomics RAST server – a public resource for the automatic phylogenetic and functional analysis of Metagenomes. *BMC Bioinformatics* 9. <https://doi.org/10.1186/1471-2105-9-386>
68. De Wit P, Pespeni MH, Ladner JT, Barshis DJ, Seneca F, Jaris H, Therkildsen NO, Morikawa M, Palumbi SR. 2012. The simple fool's guide to population genomics via RNA-seq: an introduction to high-throughput sequencing data analysis. *Mol Ecol Res* 12:1058–1067. <https://doi.org/10.1111/1755-0998.12003>
69. Langmead B, Salzberg SL. 2012. Fast gapped-read alignment with Bowtie 2. *Nat Methods* 9:357–359. <https://doi.org/10.1038/nmeth.1923>
70. Anders S, Pyl PT, Huber W. 2015. HTSeq—a python framework to work with high-throughput sequencing data. *Bioinformatics* 31:166–169. <https://doi.org/10.1093/bioinformatics/btu638>
71. Love MI, Huber W, Anders S. 2014. Moderated estimation of fold change and dispersion for RNA-seq data with DESeq2. *Genome Biol* 15:550. <https://doi.org/10.1186/s13059-014-0550-8>
72. Cook RD. 1977. Detection of influential observation in linear regression. *Technometrics* 19:15–18. <https://doi.org/10.1080/00401706.1977.10489493>
73. Benjamini Y, Hochberg Y. 1995. Controlling the false discovery rate: a practical and powerful approach to multiple testing. *J Royal Stat Soc Series B* 57:289–300. <https://doi.org/10.1111/j.2517-6161.1995.tb02031.x>
74. Kembel SW, Cowan PD, Helmus MR, Cornwell WK, Morlon H, Ackerly DD, Blomberg SP, Webb CO. 2010. Picante: R tools for integrating phylogenies and ecology. *Bioinformatics* 26:1463–1464. <https://doi.org/10.1093/bioinformatics/btq166>
75. Gregoire Taillefer A, Wheeler TA. 2018. Tracking wetland community evolution using Diptera taxonomic, functional and phylogenetic structure. *Insect Conserv Divers* 11:276–293. <https://doi.org/10.1111/icad.12271>